

Getting back to Na_xCoO_2 : spectral and thermoelectric properties

L. Boehnke¹ and F. Lechermann^{*,1}

¹ I. Institut für Theoretische Physik, Universität Hamburg, Germany

Received XXXX, revised XXXX, accepted XXXX

Published online XXXX

Key words: strong correlations, density functional theory, dynamical mean-field theory, susceptibility, thermopower

* Corresponding author: Frank.Lechermann@physnet.uni-hamburg.de

Sodium cobaltate Na_xCoO_2 as dopable strongly correlated layered material with a triangular sublattice still poses a challenging problem in condensed matter. The intriguing interplay between lattice, charge, spin and orbital degrees of freedom leads to a complex phase diagram bounded by a nominal Mott ($x=0$) regime and a band-insulating ($x=1$) phase. By means of the charge self-consistent density functional theory (DFT) plus dynamical mean-field theory (DMFT) scheme, built on a pseudopotential framework combined with a continuous-time quantum Monte-Carlo solver, we here study the one-particle spectral function $A(\mathbf{k}, \omega)$ as well as the thermopower $S(T)$.

The computations may account for the suppression of the e'_g pockets in $A(\mathbf{k}, \omega)$ at lower doping in line with photoemission experiments. Enhancement of the thermopower is verified within the present elaborate multi-orbital method to treat correlated materials. In addition, the two-particle dynamic spin susceptibility $\chi_s(\omega, \mathbf{q})$ is investigated based on a simplified tight-binding approach, yet by including vertex contributions in the DMFT linear response. Besides the identification of paramagnon branches at higher doping, a prominent high-energy antiferromagnetic mode close to $x=0.67$ is therewith identified in $\chi_s(\omega, \mathbf{q})$, which can be linked to extended hopping terms on the CoO_2 sublattice.

Copyright line will be provided by the publisher

1 Introduction The quasi two-dimensional sodium cobaltate system Na_xCoO_2 marks one milestone in the investigation of realistic strongly correlated electron systems. It consists of stacked triangular CoO_2 layers, glued together by Na ions inbetween. Depending on the doping x , the nominal oxidation state of the cobalt ion lies between $\text{Co}^{4+}(3d^5)$ and $\text{Co}^{3+}(3d^6)$. While the $x=1$ compound is a band insulator with a filled low-spin $\text{Co}(t_{2g})$ subshell, for $x=0$ a single hole resides therein. Stimulated by findings of large thermoelectric response at higher doping x [1,2] and superconductivity for $x \sim 0.3$ upon intercalation with water [3], the phase diagram of Na_xCoO_2 attracted enormous interest, both experimentally as well as theoretically, in the pre-pnictide era of the early 2000 century. The relevance of strong correlation effects due to the partially filled $\text{Co}(3d)$ shell for $x < 1$ has been motivated by several

experiments, e.g., from optics [4], photoemission [5,6,7,8] and transport [9] measurements.

Although much progress has been made in the understanding of layered cobaltates, after more than ten years of extensive research many problems are still open. We here want to address selected matters of debate, namely the nature of the low-energy electronic one-particle spectral function, the peculiarities of the dynamic spin response as well as the temperature- and doping-dependent behavior of the Seebeck coefficient.

2 Theoretical approach Effective single-particle methods based on the local density approximation (LDA) to density functional theory (DFT) are known to be insufficient to cover the rich physics of strongly correlated materials. Tailored model-Hamiltonian approaches to be treated within a powerful many-body technique such as

Copyright line will be provided by the publisher

dynamical mean-field theory (DMFT) are thus useful to reveal important insight in the dominant processes at high and low energy. Nowadays the DFT+DMFT methodology (see e.g. [10] for a review) opens the possibility to tackle electronic correlations with the benefit of the fully interlaced LDA materials chemistry.

In this work a charge self-consistent DFT+DMFT scheme [11] built up on an efficient combination of a mixed-basis pseudopotential framework [12] with a hybridization-expansion continuous-time quantum Monte-Carlo solver [13, 14, 15, 16] is utilized to retrieve spectral functions and the thermopower. Thereby the correlated subspace consists of the projected [17, 18] t_{2g} orbitals, i.e. a three-orbital many-body treatment is performed within the single-site DMFT part. The generic multi-orbital Coulomb interactions include density-density as well as spin-flip and pair-hopping terms, parametrized [19, 20] by a Hubbard $U=5$ eV and a Hund's exchange $J=0.7$ eV. Since the physics of sodium cobaltate is intrinsically doping dependent, we constructed Na pseudopotentials with fractional nuclear charge in order to cope therewith in DFT+DMFT. A simplistic structural approach was undertaken, utilizing a primitive hexagonal cell allowing for only one formula unit of Na_xCoO₂, with the fractional-charge Na in the so-called Na2 position. Thus note that therefore the bilayer splitting does not occur in the electronic structure. Our calculations are straightforwardly extendable to more complex unit cells and geometries, however the present approach suits already the purpose of allowing for some general qualitative statements.

The resulting 3×3 DFT+DMFT Green's function in Bloch space with one correlated Co ion in the primitive cell hence reads here [11]

$$\mathbf{G}^{\text{bl}}(\mathbf{k}, i\omega_n) = \left[(i\omega_n + \mu)\mathbf{1} - \varepsilon_{\mathbf{k}}^{\text{KS}} - \mathbf{P}^\dagger(\mathbf{k}) \cdot \Delta \Sigma^{\text{imp}}(i\omega_n) \cdot \mathbf{P}(\mathbf{k}) \right]^{-1}, \quad (1)$$

where $\varepsilon_{\mathbf{k}}^{\text{KS}}$ denotes the Kohn-Sham (KS) dispersion part, μ is the chemical potential and $\mathbf{P}(\mathbf{k})$ the t_{2g} projection matrix mediating between the Co correlated subspace and the crystal Bloch space. The impurity self-energy term $\Delta \Sigma^{\text{imp}}$ includes the DMFT self-energy modified by the double-counting correction. For the latter the fully-localized form [21] has been utilized. To extract the one-particle spectral function $A(\mathbf{k}, \omega) = -\pi^{-1} \text{Im} G^{\text{bl}}(\mathbf{k}, \omega)$ as well as the thermopower, an analytical continuation of the impurity self-energy term $\Delta \Sigma^{\text{imp}}$ in Matsubara space ω_n was performed via Padé approximation. Note that via the upfolding procedure within eq. (1), the resulting real-frequency self-energy term in Bloch space carries k dependence, i.e. $\Delta \Sigma^{\text{bl}} = \Delta \Sigma^{\text{bl}}(\mathbf{k}, \omega)$.

For the investigation of the thermoelectric response, the Seebeck coefficient is calculated within the Kubo formalism from

$$S = -\frac{k_B}{|e|} \frac{A_1}{A_0}, \quad (2)$$

where the correlation functions A_n are given by

$$A_n = \sum_{\mathbf{k}} \int d\omega \beta^n (\omega - \mu)^n \left(-\frac{\partial f_\mu}{\partial \omega} \right) \times \text{Tr} [\mathbf{v}(\mathbf{k})A(\mathbf{k}, \omega)\mathbf{v}(\mathbf{k})A(\mathbf{k}, \omega)]. \quad (3)$$

Here β is the inverse temperature, $\mathbf{v}(\mathbf{k})$ denotes the Fermi velocity calculated from the charge self-consistent KS part and f_μ marks the Fermi-Dirac distribution. Due to subtle refinements in the low-energy regime close to the Fermi level within the charge self-consistent DFT+DMFT scheme, computing A_n through eq. (3) for the three-orbital system at hand is quite challenging. It requires great care both in the handling of the frequency dependence of the spectral function through the analytical continuation of the local self-energy term as well as the evaluation of the k sum. The difficulty with the latter is the sharp structure of the summand especially for low temperatures. Even a tetrahedron summation is problematic due to the double appearance of the spectral function in the sum [22]. We overcome this problem by using an adaptive numerical integration method separately for each A_n , where $\Delta \Sigma^{\text{bl}}(\mathbf{k}, \omega)$, $\mathbf{v}(\mathbf{k})$ and $\varepsilon_{\mathbf{k}}^{\text{KS}}$ are linearly interpolated in reciprocal space. Since all these quantities are relatively smooth in k , the resulting A_n show only weak dependence on the underlying mesh for these interpolations.

Finally, the expensive two-particle-based dynamic spin response with relevant local vertex corrections was studied. Thereby a simplified single-band tight-binding parametrization [23] of the realistic dispersion, including hopping integrals up to third-nearest neighbor, entered the DMFT self-consistency cycle. For more details on the utilized DMFT+vertex technique see [16, 24].

3 One-particle spectral function The low-energy electronic states of Na_xCoO₂ close to the Fermi level ε_F have been subject to many discussions. LDA calculations for single-formula-unit cells reveal a threefold bandstructure of about 1.5 eV total bandwidth, dominantly originating from the Co $3d(t_{2g})$ states [25]. The resulting LDA Fermi surface (FS) consists of an a_{1g} -like hole sheet with additional e'_g -like hole pockets near the K point of the hexagonal 1. Brillouin zone (BZ). For larger doping these hole pockets become more and more filled and their existence for $x \gtrsim 0.6$ subtly depends on the very structural details [26]. Not only displays the measured spectral function $A(\mathbf{k}, \omega)$ from angle-resolved photoemission (ARPES) experiments a much narrower dispersion very close to ε_F , but also the FS at lower doping lacks the hole-pocket sheets for any doping x [6, 27, 7, 8]. Usually LDA works surprisingly well for the FS of strongly correlated metals, even if the method does not allow for the proper renormalization and the appearance of Hubbard sidebands. Hence sodium cobaltate seems to belong to rare cases of correlated metals where the LDA FS topology does not agree with experiment.

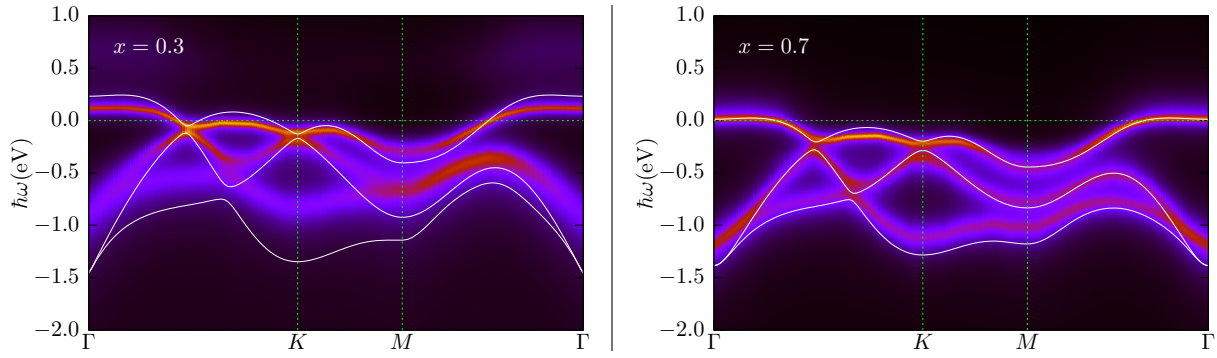


Figure 1 DFT+DMFT spectral function $A(\mathbf{k}, \omega)$ for $x=0.3$ (left) and $x=0.7$ (right) at temperature $T=290\text{K}$. For comparison the LDA band structure is drawn in white. The apical oxygen position was chosen such that an LDA single-sheet FS barely exists for $x=0.7$

Many attempts have been elaborated in order to either explain the non-existence of the hole pockets or to prove the ARPES data wrong. Without going into the very details of this rather long story, no definite final decision has been made on either line of argument. Concerning proper correlated methodologies, DFT+DMFT without charge self-consistency, i.e. in the traditional post-processing manner, may even *increase* the strength of the hole pockets (see e.g. [28]). It appeared that the size of the $a_{1g}-e'_g$ crystal-field splitting plays an important role when turning on correlations [29, 28]. From an LDA+Gutzwiller study by Wan *et al.* [30] it became clear that charge self-consistency may have a relevant influence on the correlated FS and the hole pockets indeed disappeared for $x>0.3$ in their work.

In order to touch base with these results we computed the one-particle spectral function $A(\mathbf{k}, \omega)$ within charge self-consistent DFT+DMFT for $x=0.3$ and $x=0.7$. Thereby within our simplified structural treatment the apical oxygen position was chosen such to allow for a single-sheet a_{1g} -like hole FS within LDA at $x=0.7$. Though the impact of charge order onto the spectral function is believed to be also important [31], we here neglect this influence and concentrate on the multi-orbital interplay and its impact on the correlated Fermi surface. Figure 1 shows the obtained three-orbital spectral functions close to the Fermi level. Note that there is also a lower Hubbard band, but due to the strong doping from half filling it is located in the energy range $[-6, -4]$ eV. As expected, the less-doped $x=0.3$ case shows a stronger total renormalization of the t_{2g} derived manifold. The most important observation is the clear shift of the potential pocket-forming e'_g -like quasiparticle bands away from ε_F compared to the LDA result. This here amounts to a (nearly complete) vanishing of the pockets for $x=0.3$, where they are still sizable in LDA. Even if there are some ambiguities concerning possible modifications due to structural details, the main trend that charge self-consistent DFT+DMFT (notably without invoking long-range order) tends to suppress the e'_g derived pockets is evident. Additionally the e'_g -like states exhibit a substantial broadening

also with (nearly) total filling, a multi-orbital effect discussed already for filled t_{2g} states in LaNiO_3 [32]. This altogether brings the theoretical description in line with the available ARPES data. Thus charge self-consistency can be an important ingredient in the calculations, accounting for shifts of the level structure in sensitive crystal-field environments.

4 Transport: Seebeck coefficient The increased thermoelectric response at larger doping x marks one of the Na_xCoO_2 key aspects [1, 2, 33, 34]. Although the more complex related so-called misfit cobaltates appear to display even larger thermopower and increased figure of merit (see e.g. [35] for a recent review), the sodium cobaltate system still holds most of the main physics ready in its simplest structural form. There have been various the-

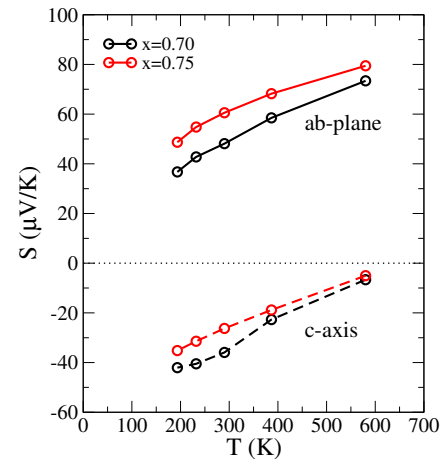


Figure 2 Seebeck coefficient $S(T)$ within charge self-consistent DFT+DMFT for larger doping. Full lines correspond to the inplane thermopower, dashed lines to $S(T)$ along the c -axis.

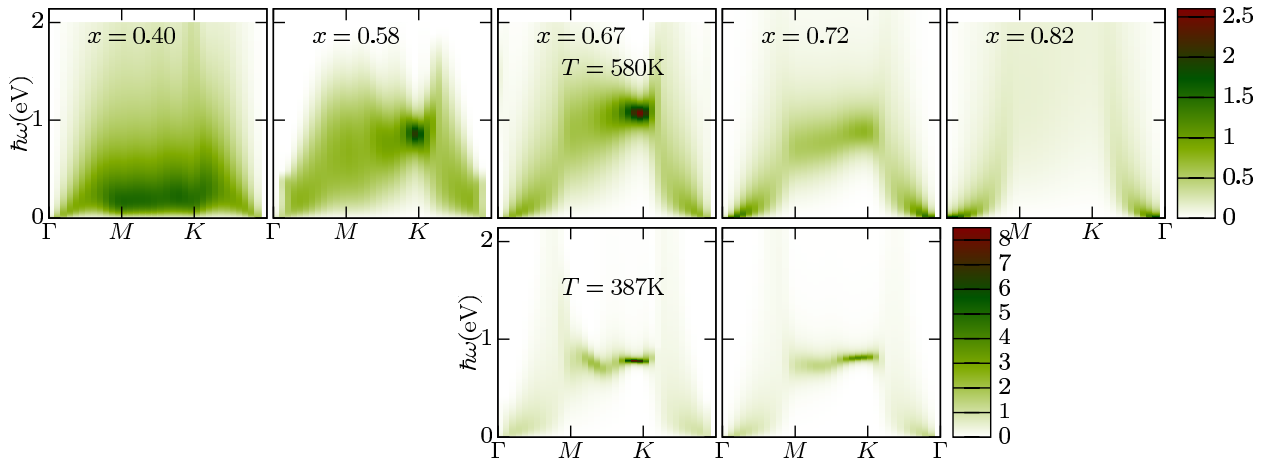


Figure 3 Doping-dependent dynamic spin susceptibility $\chi_s(\omega, \mathbf{q}, T)$. The lower row shows the results for reduced T for the same respective doping as directly above.

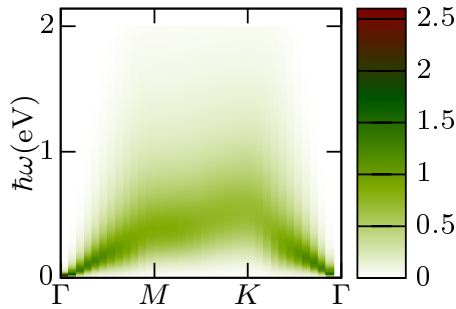


Figure 4 Dynamic spin susceptibility $\chi_s(\omega, \mathbf{q}, T=580\text{K})$ for only nearest-neighbor hopping $-t$ at $x=0.67$.

oretical modelings of the Seebeck coefficient for this system [36,37,38,39,40,41], ranging from the use of Heikes formula, Boltzmann-equation approaches as well as Kubo-formula oriented modelings. Albeit for a full account of thermoelectricity details may matter [40,41], for the doping regime $0.6 < x < 0.75$ nearly all different theoretical descriptions yield thermopower values within the ranges of the experimental data. However open modeling questions remain for the highly increased Seebeck values in the regime of vary large doping $x > 0.8$ [34,39] as well as for lower dopings $x \lesssim 0.5$, where e.g. a nonmonotonic $S(T)$ with decreasing temperature is observed [33].

Here we exhibit results for the thermopower as obtained within our charge self-consistent DFT+DMFT-based Kubo-formalism approach which builds up on the t_{2g} correlated subspace for Na_xCoO_2 . Data is provided for $x=0.7$ and $x=0.75$ in Fig. 2, the other more challenging doping regimes concerning the thermoelectric response will be addressed in future studies. For instance, we expect that the low-lying e'_g bands leave some fingerprints in the thermopower for small x . Longer-ranged FM spin

fluctuations and charge-ordering tendencies [31] may influence $S(T)$ for $x > 0.8$. Our inplane Seebeck values are in good agreement with experimental data of Kaurav *et al.* [33]. The increased response for $x=0.75$ compared to $x=0.7$ is also verified, albeit the experimental tendency towards stronger enhancement with increased doping is still somewhat underestimated from theory. In addition to the inplane values, Fig. 2 depicts the $S(T)$ tensor part along the c -axis of the system. Besides the n -like response with a change of sign, the absolute value becomes reduced at larger T , related to the different (rather incoherent) transport between layers at elevated temperature [5].

5 Two-particle function: dynamic spin susceptibility Besides the one-particle spectral properties and the thermopower, a further intriguing cobaltate issue is the magnetic behavior with doping. Within the frustrated triangular CoO_2 layers superexchange may dominate the low-doping regime due to nominal Mott proximity, but competing exchange processes set in at larger doping. The work by Lang *et al.* [42] based on nuclear-magnetic-resonance measurements nicely summarized the magnetic phase diagram of Na_xCoO_2 with temperature T , showing the in-plane crossover from antiferromagnetic (AFM) to ferromagnetic (FM) correlations with the eventual onset of A-type AFM order for $x > 0.75$.

In line with the results for the spectral function we computed the spin susceptibility $\chi_s(\omega, \mathbf{q}, T)$ for an effective single-band model using DMFT with local vertex contributions [24]. This allows for the theoretical verification of the AFM-to-FM crossover. It can directly be retrieved from the shift of maxima in the static part $\chi_s(\omega=0, \mathbf{q}, T)$ for \mathbf{q} at the BZ K point at small x towards maxima at $\mathbf{q}=0$ (Γ point) at larger doping. Figure 3 displays the full dynamic spin susceptibility with increasing x in the paramagnetic regime. Below $x=0.5$ the strong two-particle spectral

intensity close to M and K at the BZ boundary is indeed visible. For rather large doping the intensity accumulates at small frequency ω near the Γ point, with clear paramagnon branches due to the proximity towards inplane FM order. We note that the vertex contributions are essential for the qualitative as well as quantitative signatures in the doping-dependent spin susceptibility [24].

Most interestingly, there also is a high-intensity mode near the K point with maximum spectral weight well located around the comensurable doping $x=0.67$ on the frustrated CoO_2 triangular lattice. The corresponding excitation energy of about 1 eV for $T=580\text{K}$ is decreasing with lowering the temperature. Thus albeit the low-energy spin excitations for that larger doping have already shifted towards FM kind, a rather stable finite- ω AFM-like mode becomes available. This intriguing doping and frequency dependence of the effective exchange J can be linked to the specific hopping-integral structure of sodium cobaltate. In this respect Fig. 4 shows the dynamic spin susceptibility at $x=0.67$ for the Hubbard model on the triangular lattice with only nearest-neighbor hopping $-t$. While the FM paramagnon modes close to Γ seem even strengthened in that case, the high-energy feature close to K is now completely absent. Still it is not obvious to draw a straightforward connection between the one-particle spectral function and two-particle dynamic spin susceptibility.

6 Summary We have presented a state-of-the-art DFT+DMFT investigation of the multi-orbital one-particle spectral properties as well as the thermoelectric behavior of Na_xCoO_2 . The charge self-consistent scheme brings the one-particle spectral function concerning the correlated Fermi surface and the broadening of the occupied part in good agreement with available ARPES data. Further extensions of the realistic methodology towards the proper inclusion of charge-order effects, eventually with incorporating relevant intersite Coulomb terms, are still needed for a comprehensive understanding. Nonetheless the present framework is capable of addressing the temperature- and doping-dependent thermopower in line with experimental data for the larger doping regime. Detailed studies of the more critical regions in this respect at low and very high dopings are envisaged. Through the inclusion of sophisticated vertex contributions in a simplified tight-binding-based approach, details of the dynamic spin susceptibility, e.g. the prediction of a rather stable high-energy AFM-like mode close to $x=0.67$, have been revealed. Additional experimental work is needed to verify our results and to stimulate future work. Eventually, the investigation of the direct impact of two-particle correlations on the one-particle spectrum is a challenging goal, but therefore it will be necessary to go beyond the local-correlation viewpoint of DMFT.

Acknowledgements We thank D. Grieger, A. I. Lichtenstein and O. E. Peil for helpful discussions. Financial support from the DFG-SPP1386 and the DFG-FOR1346 is acknowl-

edged. Computations were performed at the local computing center of the University of Hamburg as well as the North-German Supercomputing Alliance (HLRN) under the grant hhp00026.

References

- [1] I. Terasaki, Y. Sasago, and K. Uchinokura, *Phys. Rev. B* **56**, R12685 (1997).
- [2] T. Motohashi, E. Naujalis, R. Ueda, K. Isawa, M. Karppinen, and H. Yamauchi, *Appl. Phys. Lett.* **79**, 1480 (2001).
- [3] K. Takada, H. Sakurai, E. Takayama-Muromachi, F. Izumi, R. A. Dilanian, and T. Sasaki **422**, 53 (2003).
- [4] N.L. Wang, P. Zheng, D. Wu, Y. C. Ma, T. Xiang, R. Y. Jin, and D. Mandrus, *Phys. Rev. Lett.* **93**, 237007 (2004).
- [5] T. Valla, P.D. Johnson, Z. Yusof, B. Wells, Q. Li, S. M. Loureiro, R. J. Cava, M. Mikami, M. Y. Y. Mori, and T. Sasaki **417**, 627 (2002).
- [6] M. Z. Hasan, Y.D. Chuang, D. Qian, Y. W. Li, Y. Kong, A. Kuprin, A. V. Fedorov, R. Kimmerring, E. Rotenberg, K. Rossnagel, Z. Hussain, H. Koh, N. S. Rogado, M. L. Foo, and R. J. Cava, *Phys. Rev. Lett.* **92**, 246402 (2004).
- [7] H. B. Yang, Z. Wang, and H. Ding, *J. Phys.: Condens. Matter* **19**, 355004 (2007).
- [8] J. Geck, S. V. Borisenko, H. Berger, H. Eschrig, J. Fink, M. Knupfer, K. Koepfner, A. Koitzsch, A. A. Kordyuk, V. B. Zabolotnyy, and B. Büchner, *Phys. Rev. Lett.* **99**, 046403 (2007).
- [9] M. L. Foo, Y. Wang, S. Watauchi, H. W. Zandbergen, T. He, R. J. Cava, and N. P. Ong, *Phys. Rev. Lett.* **92**, 247001 (2004).
- [10] G. Kotliar, S. Y. Savrasov, K. Haule, V. S. Oudovenko, O. Parcollet, and C. A. Marianetti, *Rev. Mod. Phys.* **78**, 865 (2006).
- [11] D. Grieger, C. Piefke, O. E. Peil, and F. Lechermann, *Phys. Rev. B* **86**, 155121 (2012).
- [12] B. Meyer, C. Elsässer, F. Lechermann, and M. Fähnle, FORTRAN 90 Program for Mixed-Basis-Pseudopotential Calculations for Crystals, Max-Planck-Institut für Metallforschung, Stuttgart, unpublished.
- [13] A. N. Rubtsov, V. V. Savkin, and A. I. Lichtenstein, *Phys. Rev. B* **72**, 035122 (2005).
- [14] P. Werner, A. Comanac, L. de' Medici, M. Troyer, and A. J. Millis, *Phys. Rev. Lett.* **97**, 076405 (2006).
- [15] M. Ferrero and O. Parcollet, TRIQS: a Toolbox for Research in Interacting Quantum Systems.
- [16] L. Boehnke, H. Hafermann, M. Ferrero, F. Lechermann, and O. Parcollet, *Phys. Rev. B* **84**, 075145 (2011).
- [17] B. Amadon, F. Lechermann, A. Georges, F. Jollet, T. O. Wehling, and A. I. Lichtenstein, *Phys. Rev. B* **77**, 205112 (2008).
- [18] V. I. Anisimov, D. E. Kondakov, A. V. Kozhevnikov, I. A. Nekrasov, Z. V. Pchelkina, J. W. Allen, S. K. Mo, H. D. Kim, P. Metcalf, S. Suga, A. Sekiyama, G. Keller, I. Leonov, X. Ren, and D. Vollhardt, *Phys. Rev. B* **71**, 125119 (2005).
- [19] C. Castellani, C. R. Natoli, and J. Ranninger, *Phys. Rev. B* **18**, 4945 (1978).
- [20] R. Frésard and G. Kotliar, *Phys. Rev. B* **56**, 12909 (1997).
- [21] V. I. Anisimov, I. V. Solovyev, M. A. Korotin, M. T. Czyżyk, and G. A. Sawatzky, *Phys. Rev. B* **48**, 16929 (1993).

- [22] G. Palsson, Computational studies of thermoelectricity in strongly correlated electron systems, PhD thesis, New Brunswick, Rutgers, The State University of New Jersey, 2001.
- [23] H. Rosner, S. L. Drechsler, G. Fuchs, A. Handstein, A. Wälte, and K. H. Müller, *Braz. J. Phys.* **33**, 718 (2003).
- [24] L. Boehnke and F. Lechermann, *Phys. Rev. B* **85**, 115128 (2012).
- [25] D. Singh, *Phys. Rev. B* **61**, 13397 (2000).
- [26] M. D. Johannes, D. A. Papaconstantopoulos, D. J. Singh, and M. J. Mehl, *Europhys. Lett.* **68**, 433 (2004).
- [27] D. Qian, L. Wray, D. Hsieh, L. Viciu, R. J. Cava, J. L. Luo, D. Wu, N. L. Wang, and M. Z. Hasan.
- [28] C. A. Marianetti, K. Haule, and O. Parcollet, *Phys. Rev. Lett.* **99**, 246404 (2007).
- [29] F. Lechermann, S. Biermann, and A. Georges, *Progress of Theoretical Physics Supplement* **160**, 233 (2005).
- [30] G. T. Wang, X. Dai, and Z. Fang, *Phys. Rev. Lett.* **101**, 066403 (2008).
- [31] O. E. Peil, A. Georges, and F. Lechermann, *Phys. Rev. Lett.* **107**, 236404 (2011).
- [32] X. Deng, M. Ferrero, J. Mravlje, M. Aichhorn, and A. Georges, *Phys. Rev. B* **85**, 125137 (2012).
- [33] N. Kaurav, K. K. Wu, Y. K. Kuo, G. J. Shu, and F. C. Chou, *Phys. Rev. B* **79**, 075105 (2009).
- [34] M. Lee, L. Viciu, L. Li, Y. Wang, M. L. Foo, S. Watauchi, R. A. Pascal, R. J. Cava, and N. P. Ong, *Nat. Mat.* **5**, 537 (2006).
- [35] S. Hébert, W. Kobayashi, H. Muguerra, Y. Bréard, N. Raghavendra, F. Gascoin, E. Guilmeau, and A. Maignan, *Phys. Status Solidi A* **210**, 69 (2013).
- [36] W. Koshibae and S. Maekawa, *Phys. Rev. Lett.* **87**, 236601 (2001).
- [37] N. Hamada, T. Imai, and H. Funashima **19**, 365221 (2007).
- [38] K. Kuroki and R. Arita, *J. Phys. Soc. Jpn.* **76**, 083707 (2007).
- [39] M. R. Peterson, B. S. Shastry, and J. O. Haerter, *Phys. Rev. B* **76**, 165118 (2007).
- [40] P. Wissgott, A. Toschi, H. Usui, K. Kuroki, and K. Held, *Phys. Rev. B* **82**, 201106(R) (2010).
- [41] G. Sangiovanni, P. Wissgott, F. Assaad, A. Toschi, and K. Held, *Phys. Rev. B* **86**, 035123 (2012).
- [42] G. Lang, J. Bobroff, H. Alloul, G. Collin, and N. Blanchard, *Phys. Rev. B* **78**, 155116 (2008).